Acta Cryst. (1990). B46, 1–7

Experimental and Theoretical Deformation Electron Density for Vanadyl Sulfate Hexahydrate

BY M. HJORTH, R. NORRESTAM AND H. JOHANSEN

Chemistry Department B, DTH 301, *The Technical University of Denmark, DK*-2800 *Lyngby, Denmark*

(*Received* 27 *December* 1988; *accepted* 3 *April* 1989)

Abstract

Pentaaquaoxovanadium(IV) sulfate monohydrate, $[VO(H_2O)_5]^{2+}[SO_4]^{2-}.H_2O$, $M_r = 271{\cdot}09$, triclinic, $P\bar{1}$, $a = 6{\cdot}190\ (1)$, $b = 7{\cdot}471\ (1)$, $c = 10{\cdot}100\ (1)$ Å, $\alpha = 92{\cdot}28\ (1)$, $\beta = 101{\cdot}96\ (1)$, $\gamma = 95{\cdot}35\ (1)°$, $V = 454{\cdot}1\ (1)$ Å^3, $Z = 2$, $D_x = 1{\cdot}983\ (1)$ g cm^{-3}, λ(Mo $K\alpha$) = 0·71073 Å, $\mu = 13{\cdot}2$ cm^{-1}, $F(000) = 258$, $T = 120\ (1)$ K. Single-crystal X-ray data with aspherical multipole expansion of the electron density gave $R(F^2) = 0{\cdot}0177$ for 3367 observed unique reflections with $\sin\theta/\lambda < 0{\cdot}79$ Å^{-1}. Experimental deformation densities were calculated using thermal parameters from high-angle X-ray refinement ($0{\cdot}79 < \sin\theta/\lambda < 1{\cdot}20$ Å^{-1}). The densities have been compared with corresponding theoretical results obtained from *ab initio* calculations of multi-configurational self-consistent-field type, using an extended Gaussian basis set. Densities for the V—O bond, the oxygen lone pairs and the non-bonding *d* electron compare favorably on the qualitative level. There are quantitative differences, some of which may be explained by thermal smearing.

Introduction

The electron density distribution in the vanadyl ion has been studied by experimental and theoretical methods in order to get a better understanding of transition-metal complexes with few *d* electrons. Systems with more than half-filled *d* shells have previously been extensively studied *e.g.* Johansen (1976) and Toriumi & Saito (1983). It is, however, expected that there will be significant differences in the electron distributions between the electron-rich and the electron-poor transition metals, since such a trend is already found in the first row of the periodic system. As an example, a chemically clear picture is usually obtained when dealing with carbon, whereas oxygen and fluorine lead to less easily characterized features, where elaborate promolecules have to be used as reference systems in order to enhance the chemical concepts (Hall, 1986).

The vanadyl ion has a strong bond with both σ and π character. It is formally a d^1 system, which participates as a cation in many compounds. The pentaaquavanadyl ion, $VO(H_2O)_5^{2+}$, was selected as having neutral ligands together with a saturated coordination sphere for vanadium. The system appears to be well suited to expose different aspects of bonds between transition metals and their ligands.

Different types of hydrated vanadyl ions in the solid state have earlier been observed in *e.g.* sulfates. These include a trihydrate (Théobald & Galy, 1973), two pentahydrates (Tachez, Théobald, Watson & Mercier, 1979; Tachez & Théobald, 1980*b*) and a hexahydrate (Tachez & Théobald, 1980*a*). The hexahydrate which contains the pentaaquavanadyl ion $VO(H_2O)_5^{2+}$ crystallizes in the centrosymmetric space group $P\bar{1}$ and appears to be a suitable specimen to provide accurate X-ray data on the octahedrally coordinated $VO(H_2O)_5^{2+}$ ion.

Experimental

Highly hygroscopic, dark-blue crystals of $VOSO_4.6H_2O$ were prepared by evaporation of a solution of 0·65 g commercial $VOSO_4.5H_2O$ in 1 ml water at room temperature until crystallization had started; evaporation was then continued in a refrigerator (~278 K). Suitable crystals were obtained after approximately one week.

Single-crystal X-ray intensity data were collected at 120 (1) K with an Enraf–Nonius CAD-4 diffractometer using a conventional nitrogen gas stream cooling device. The centrosymmetric triclinic space-group symmetry used by Tachez & Théobald (1980*a*) was confirmed by the present study. Further experimental conditions are given in Table 1. Crystal dimensions used for the absorption correction were verified by a statistical analysis of intensities collected by ψ scans for 26 reflections.

The e.s.d.'s of the corrected intensities were estimated as $\sigma^2(I) = [k\sigma_c(I)]^2 + (kPI)^2$, where the index *c* refers to counting statistics, *P* is the instability constant and *k* is the time-dependent scale factor on the intensities (McCandlish, Stout & Andrews, 1975). The values of *P* and *k* [$P = 0{\cdot}00779$, $k = (1 + 0{\cdot}656 \times 10^{-4}t)^{-1}$ for $t < 52{\cdot}5$ (h) and $k = (1 + 0{\cdot}152 \times 10^{-4}t - 0{\cdot}0560)^{-1}$ for $t \geq 52{\cdot}5$ (h)] were obtained by linearizing the time dependence of the three intensity

0108-7681/90/010001-07$03.00

Table 1. *Experimental conditions for the crystal structure determination of* $VOSO_4.6H_2O$

Crystal shape	Prismatic
Crystal size (mm)	0·30 × 0·085 × 0·065
Determination of unit cell	
No. of reflections used	21
θ range (°)	12·4 to 17·2
Intensity-data collection	
Maximum $\sin\theta/\lambda$ (Å^{-1})	0·79
Range of h, k and l	−9 to 9, −11 to 11 and −15 to 15
Standard reflections	$42\bar{1}$, $11\bar{8}$ and $33\bar{2}$
Intensity instability (%)	< 4
No. of collected reflections	8244
No. of unique reflections	3702
No. of observed reflections	3367
R_{int}	0·0127
Criterion for significance	$I > 3\sigma(I)$
Absorption correction	
Linear absorption coefficient (cm^{-1})	13·2
Transmission-factor range	0·81 to 0·85
Structure refinement	
Minimization	Sum of $w(\Delta F^2)^2$
Isotropic thermal parameters	H
Anisotropic thermal parameters	V, S and O
Multipole expansions	All atoms (*cf. Experimental*)
Extinction (isotropic type I)	2·9 (1) × 10^3
Maximum correction	1·22
No. of refined parameters	255
Weighting scheme	$(\sigma_{F^2})^{-2}$ (*cf. Experimental*)
Final R	0·0177
Final wR	0·0251
Final S	2·32
Final $(\Delta/\sigma)_{max}$	0·24

control reflections. A normal probability plot (Abrahams, 1974) of the observed deviations of the corrected intensities is shown in Fig. 1.

The coordinates of Tachez & Théobald (1980*a*) were used as the starting point for the present structure determination. A least-squares refinement yielded the R value 0·027 ($wR = 0·046$) on F^2, with anisotropic thermal displacements for the non-H atoms and isotropic ones for the H atoms. The number of parameters, including an isotropic extinction parameter, was 162 and the number of observations included (*cf.* Table 1) 3314 [$I > 5\sigma(I)$].

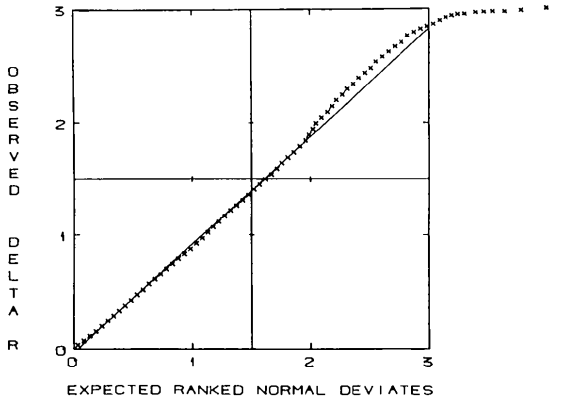

Fig. 1. Normal probability plot of the deviations of the symmetry-dependent observed intensities (F^2_{obs}) from their average (F^2_{av}), $\Delta R = |F^2_{obs} - F^2_{av}|/\sigma$. Every hundredth reflection is marked by an ×. The least-squares line has the slope 0·95 and the intersection −0·04.

The final refinement was based on a multipole expansion of the electron density. An analytical expression for the electron density with multipoles up to the fourth order (hexadecapoles) is

$$\rho(\mathbf{r}) = \rho_{sph}(r) + P_v\kappa'^3\rho_{valence}(\kappa' r) + \sum_{l=0}^{4}\kappa''^3 R_l(\kappa'' r)\sum_{m=-l}^{l} P_{lm}Y_{lm}(\mathbf{r}/r). \quad (1)$$

The radial functions, R_l, and the spherical harmonics, Y_{lm}, are described in detail by *e.g.* Kurki-Suonio (1977) and Hansen & Coppens (1978). A fourth-order multipole expansion gives 26 parameters for each atom if no symmetry restrictions are adopted. Symmetry restrictions used in this work are discussed below. The final atomic coordinates and isotropic thermal parameters are listed in Table 2.* The temperature factors for the non-H atoms were refined from high-angle X-ray data with $0·79 < \sin\theta/\lambda < 1·20$ Å^{-1}, using 4491 reflections with $I > 3\sigma(I)$ giving the R value 0·064 ($wR = 0·077$) on F^2.

Programs used were *CADABS* (Norrestam, 1976) for analysis of ψ scans, *ABSCAD* (Lundgren, 1985) for absorption correction, *LSQLIN* (Lundgren, 1985) for intensity correction, *MOLLY* (Hansen & Coppens, 1978) for refinements, and *MOLPLOT* (Johansen, 1986) for contour plotting. Atomic scattering factors for V^{3+}, S and O^- for the vanadyl oxygen, O for all other oxygens, and H were from *International Tables for X-ray Crystallography* (1974).

Theoretical calculations

The theoretical calculations were made before the experimental study, and they are therefore based upon the geometry found by Tachez & Théobald (1980*a*). Some symmetry adaptation was used in order to facilitate the calculations. C_{2v} was enforced, and all the equatorial water ligands were kept in planes perpendicular to the equatorial plane.* A preliminary investigation of the VO part of the system is given by Johansen & Tanaka (1985), and a more thorough account of the calculations will be published elsewhere in connection with a study of the spectroscopic states, but some of the more important details may be of interest here.

* Lists of structure factors, anisotropic thermal parameters, deformation function parameters and coordinates for the theoretical calculations have been deposited with the British Library Document Supply Centre as Supplementary Publication No. SUP 52115 (23 pp.). Copies may be obtained through The Executive Secretary, International Union of Crystallography, 5 Abbey Square, Chester CH1 2HU, England.

Table 2. *Fractional coordinates and isotropic temperature factors*

For the non-H atoms U_{iso} has been estimated as $\frac{1}{3}\sum U_{ij}a_i^*a_j^*\mathbf{a}_i.\mathbf{a}_j$.

	x	y	z	U_{iso}(Å^2)
V	0·07586 (2)	0·26877 (2)	0·28451 (1)	0·00714 (3)
S	0·43404 (2)	0·23059 (2)	0·82726 (1)	0·00807 (3)
O(1)	0·04719 (7)	0·16986 (6)	0·41830 (5)	0·0160 (1)
O(2)	0·11718 (7)	0·04615 (6)	0·17385 (5)	0·0125 (1)
O(3)	−0·24750 (7)	0·23536 (5)	0·18798 (4)	0·0098 (1)
O(4)	0·40551 (7)	0·33949 (6)	0·34774 (5)	0·0137 (1)
O(5)	0·13327 (7)	0·38351 (6)	0·10020 (5)	0·0112 (1)
O(6)	0·02624 (7)	0·52339 (6)	0·33218 (5)	0·0133 (1)
O(7)	0·32188 (7)	0·80923 (8)	0·45455 (5)	0·0123 (1)
O(8)	0·37631 (6)	0·36973 (5)	0·72987 (5)	0·0132 (1)
O(9)	0·64123 (7)	0·29388 (6)	0·92564 (5)	0·0141 (1)
O(10)	0·25191 (7)	0·18445 (6)	0·89725 (5)	0·0161 (1)
O(11)	0·47304 (6)	0·06504 (5)	0·75052 (4)	0·0117 (1)
H(21)	0·016 (2)	−0·028 (1)	0·155 (1)	0·025 (3)
H(22)	0·235 (2)	0·003 (1)	0·188 (1)	0·035 (3)
H(31)	−0·287 (1)	0·249 (1)	0·109 (1)	0·029 (3)
H(32)	−0·323 (2)	0·147 (2)	0·203 (1)	0·035 (3)
H(41)	0·466 (2)	0·418 (2)	0·318 (1)	0·043 (3)
H(42)	0·483 (2)	0·294 (1)	0·411 (1)	0·028 (3)
H(51)	0·170 (2)	0·321 (2)	0·044 (1)	0·022 (3)
H(52)	0·184 (2)	0·478 (2)	0·096 (1)	0·031 (3)
H(61)	0·117 (2)	0·598 (1)	0·371 (1)	0·027 (3)
H(62)	−0 093 (2)	0·557 (1)	0·311 (1)	0·033 (3)
H(71)	0·380 (2)	0·853 (2)	0·403 (1)	0·024 (4)
H(72)	0·256 (2)	0·879 (2)	0·478 (1)	0·025 (4)

The calculations are all-electron *ab initio* calculations in a multi-configurational self-consistent-field (MC SCF) framework. The basis set is double-zeta quality for inner shells as well as for the valence orbitals of the water ligands, and triple-zeta quality for the valence orbitals of the vanadyl part. The 4*s* shell on vanadium is represented by two orbitals, the 4*p* by one, and the 3*d* set contains a diffuse function. The number of configuration state functions used to describe the $^2B_2$ ground state in the MC SCF calculation was 1536. C_{4v} notation has here been applied since the H atoms of the axial water ligand do not lower the symmetry very much. The main configuration is $\cdots(8a_1)^2(3e)^4(1b_2)^1$, where $8a_1$ represents the vanadyl σ bond, $3e$ the π bond, and $1b_2$ the localized d^1 electron. The weight for the main configuration in the expansion is 86%.

Discussion

Structural description

The structure found in the present investigation (Fig. 2) agrees with that found earlier by Tachez & Théobald (1980*a*). Thus, the structure is composed of $VO(H_2O)_5^{2+}$ ions, SO_4^{2-} ions and an H_2O molecule. These entities (shown in Fig. 3, together with the atomic labels used) are held together in the crystal structure by an extensive net of hydrogen bonds. Except for one of the hydrogen bonds, the O···O and H···O distances found in the present study range from 2·646 (1) to 2·794 (1) Å and from 1·85 (2) to 2·04 (2) Å, respectively. The corresponding range of the O—H···O angles is 169 (1) to 177 (1)°. As discussed by Tachez & Théobald (1980*a*) in their detailed analysis of the hydrogen-bond scheme, one of the water H atoms, H(72), participates in a weaker and possibly bifurcated hydrogen bond between O(7) and two symmetry-related O(1) atoms giving O···O distances in the present study of 2·856 (1) and 3·311 (1) Å.

The coordination octahedron formed by the O atoms around the V atom has an approximate C_{4v} symmetry, with the rotation axis passing through the water oxygen O(5), the V atom and the vanadyl oxygen O(1). The V atom is displaced 0·28 Å out of the least-squares plane through O(2), O(3), O(4) and O(6) along the fourfold axis towards O(1). The V—O bond distances to these four oxygens are almost equal, ranging from 2·010 (1) to 2·032 (1) Å (Table 3). The axial bond between the V atom and the water oxygen, O(5), is considerably longer *viz* 2·161 (1) Å. The short bond to the vanadyl oxygen is 1·600 (1) Å.

The sulfate group is close to tetrahedral (Table 3). Three of the S—O bond lengths are within three e.s.d.'s from 1·475 Å, whereas the fourth bond S—O (11) is significantly longer, 1·499 (1) Å. This difference is apparently due to hydrogen-bond effects. The oxygen atom O(11) participates in three hydrogen bonds, whereas the other three oxygens of the sulfate group participate in two hydrogen bonds.

The H—O—H bond angles in the six water molecules range from 106 (1) to 115 (1)° and the O—H

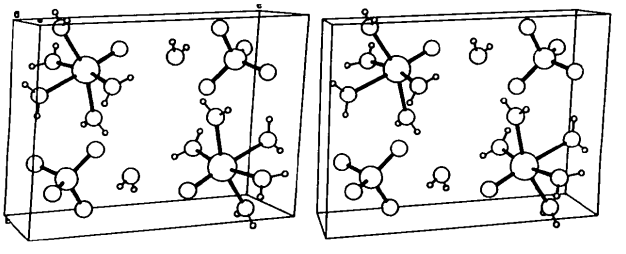

Fig. 2. Stereoscopic packing diagram of the $VO(H_2O)_5SO_4.H_2O$ structure with the *c* axis horizontal and the *b* axis vertical.

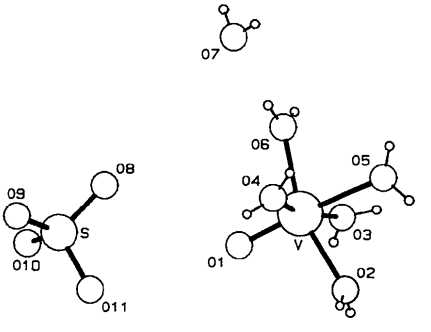

Fig. 3. The molecules of the fundamental unit together with the atomic labels used in the present study.

Table 3. *Distances* (Å) *and angles* (°) *around the* V *and* S *atoms*

V—O(1)	1·600 (1)	S—O(8)	1·477 (1)
V—O(2)	2·032 (1)	S—O(9)	1·475 (1)
V—O(3)	2·024 (1)	S—O(10)	1·472 (1)
V—O(4)	2·021 (1)	S—O(11)	1·499 (1)
V—O(5)	2·161 (1)		
V—O(6)	2·010 (1)		
O(1)—V—O(2)	96·93 (4)	O(8)—S—O(9)	109·87 (3)
O(1)—V—O(3)	97·29 (3)	O(8)—S—O(10)	110·83 (3)
O(1)—V—O(4)	95·26 (3)	O(8)—S—O(11)	108·40 (4)
O(1)—V—O(5)	174·76 (4)	O(9)—S—O(10)	110·79 (4)
O(1)—V—O(6)	102·10 (4)	O(9)—S—O(11)	108·13 (3)
O(2)—V—O(3)	87·22 (3)	O(10)—S—O(11)	108·74 (3)
O(2)—V—O(4)	93·65 (2)		
O(2)—V—O(5)	78·50 (3)		
O(2)—V—O(6)	160·61 (3)		
O(3)—V—O(4)	167·23 (3)		
O(3)—V—O(5)	85·12 (3)		
O(3)—V—O(6)	86·69 (3)		
O(4)—V—O(5)	82·57 (3)		
O(4)—V—O(6)	88·35 (2)		
O(5)—V—O(6)	82·69 (3)		

bond distances from 0·75 (2) to 0·82 (2) Å. The orientations of the water molecules coordinating the V atom are such that the planes through the water molecules at each of the four oxygens O(2), O(4), O(6) and O(3), alternate between being almost coplanar and almost perpendicular to the plane through those oxygens. Thus, the $VO(H_2O)_5^{2+}$ entity has an approximate C_{2v} symmetry rather than C_{4v}, if the H-atom positions are considered as well. The angles between the V—O bonds and the planes through the coordinating water molecules are within the range 146 (1) to 177 (1)°.

Deformation densities

As discussed above, the final refinement is based on fourth-order multipole expansion of the experimental electron density. The following point symmetries are imposed on the atomic centers: vanadium C_1, sulfur T_d, oxygen C_{2v}, hydrogen $C_{\infty v}$. The local Cartesian coordinate systems, used to describe the site symmetries, are selected so that for the S atom the three axes approximately bisect the O—S—O angles of the sulfate ion. For the sulfate and vanadyl O atoms the twofold axes are chosen along the O—S and O—V bonds, respectively. The twofold axes of the water molecules bisect the H—O—H angles. For the hydrogens the rotation axes coincide with the O—H bonds. These symmetry constraints limit the number of deformation functions to 25 for V, three for S, nine for O and five for H, as only one monopole function (the valence monopole) is used. The values of n_l in the analytical expression (*cf.* Hansen & Coppens, 1978) of the radial function $R_l(r)$ of (1) were chosen as 1, 2, 2, 3, 4, for the multipoles of order 0, 1, 2, 3, 4 of the O and H atoms, and as 4, 4, 4, 6, 8 for the S and V atoms. The exponents in $R_l(r)$ are kept equal for orders $l \geq 1$.

The experimental dynamic deformation electron densities, $\rho_{dyn} = \rho_{def} - \rho_{sph}$, are shown in Fig. 4 for some relevant planes through the $VO(H_2O)_5^{2+}$ ion. ρ_{def} is the density described by the extended model including deformation functions and ρ_{sph} is the density calculated with conventional atomic scattering factors using the high-angle thermal parameters (*cf. Experimental*). To indicate the effectiveness of the extended model to approximate the experimentally observed density, a residual map $\rho_{res} = \rho_{obs} - \rho_{def}$ is shown in Fig. 5. The largest values of ρ_{res} (about 0·1 e Å^{-3}) in the $VO(H_2O)_5^{2+}$ ion occur in the lone-pair region of the O atoms (*cf.* Fig. 5).

The ρ_{dyn} map through V and perpendicular to the vanadyl V—O bond (Fig. 4*a*) indicates substantial electron density maxima (about 0·45 e Å^{-3}) close to the nucleus atom in regions corresponding to the non-bonding *d*-electron of the V atom (*cf.* below for a comparison with the theoretical deformation density). The positions of the maxima are related by an approximate fourfold symmetry. The deviations from the fourfold symmetry can possibly be related to the alternating orientations of the water molecules at O(2), O(4), O(6) and O(3) discussed above. Density minima are found in regions towards the four ligands, but their depths alternate again, and we find two minima at $-0{\cdot}45$ e Å^{-3} and two at about $+0{\cdot}05$ e Å^{-3}.

Along the V—O bonds to the water ligands there are maxima (about 0·2 e Å^{-3}) in the ρ_{dyn} maps (Figs. 4*a–c*) at the lone-pair regions of the oxygens and as expected somewhat higher maxima (0·4 e Å^{-3}) along the shorter vanadyl V—O(1) bond. The deformation densities at the water molecules are in general agreement with the observations by Hermansson (1985) and others. Thus, the maxima corresponding to the oxygen lone pairs occur in planes perpendicular to the H—O planes, indicating an approximately tetrahedral distribution of the 'valence' electrons of the O atoms. The features are, however, not very distinct, and any significant accumulation of density on the O—H bonds is not observed. The description of the metal–water interaction is quite comparable to similar investigations with Mg, Ni and Cu as central atoms (Maslen, Ridout & Watson, 1988; Maslen, Watson & Moore, 1988).

A quantitative interpretation of the experimental maps is not straightforward, since the results are subject to thermal smearing, series-termination effects in the Fourier summation and experimental errors in the measuring and scaling of the intensities. The experimental errors have little influence, except near the atomic nuclei, where the errors will add up (Rees, 1978). The series-termination effects at the resolution of $\sin\theta/\lambda = 0{\cdot}79$ Å^{-1} will also be of minor importance, except near the nuclei (Breitenstein, Dannöhl, Meyer, Schweig & Zittlau, 1982), and in

both cases the effect is most pronounced for the heavy elements. Thus, it is concluded that thermal smearing is the main cause of error, except near the atomic centers (especially near the vanadium nucleus).

Static deformation density maps for the theoretical calculations are shown in Fig. 6. Contours are the same as in the experimental maps, but only levels with absolute values below 1 e $Å^{-3}$ have been shown. The features in the maps are more distinct

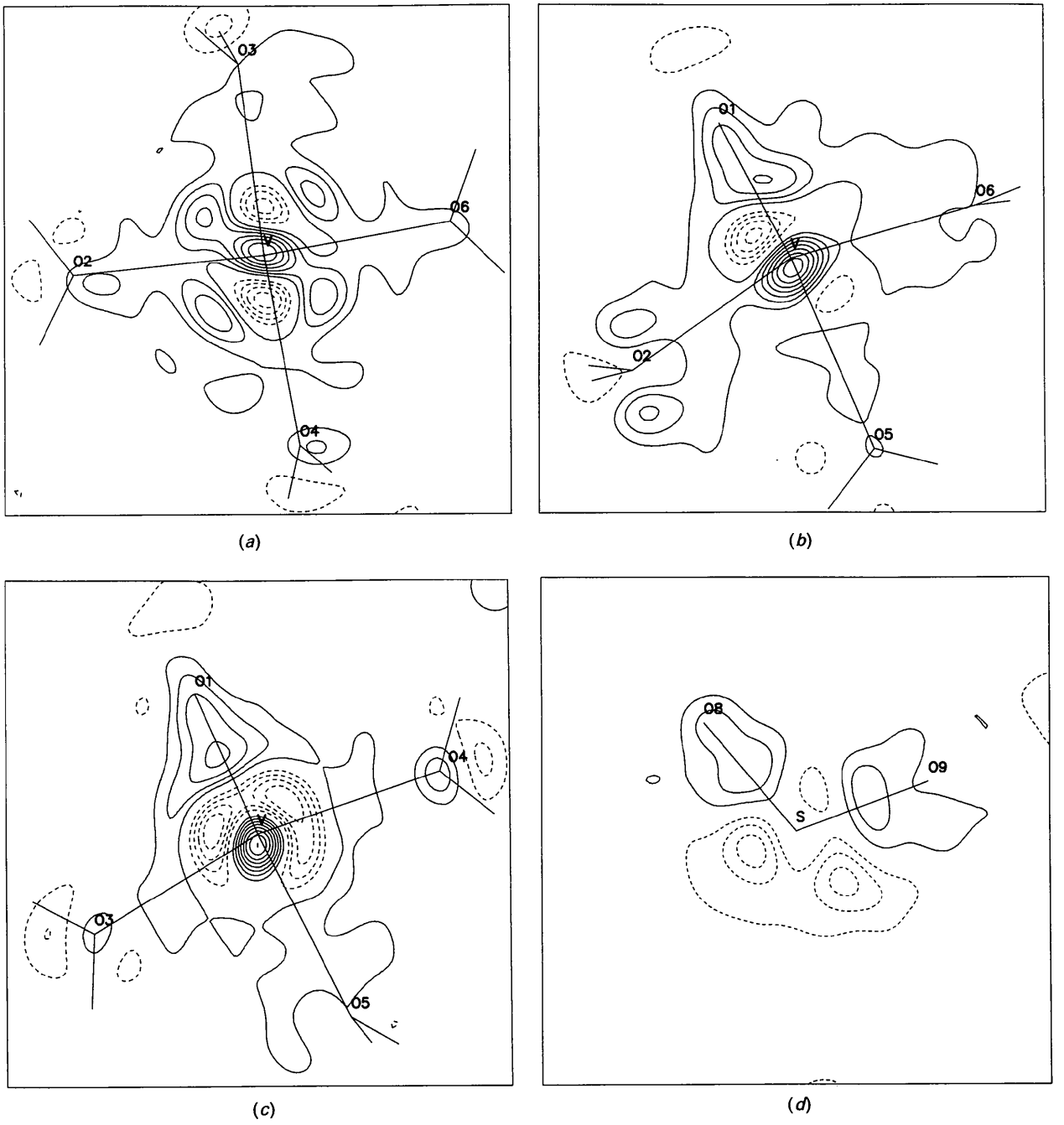

Fig. 4. Experimental dynamic deformation electron densities, $\rho_{def} - \rho_{sph}$. ρ_{def} is the electron density described by the extended model including the deformation functions, and ρ_{sph} the density calculated with usual spherical atomic scattering factors: (*a*) shows the electron densities through vanadium in the plane perpendicular to the V—O bond, (*b*) and (*c*) the densities in the planes containing the V—O bond and three water O atoms; (*d*) shows the electron densities for the sulfate group in a plane through the S and two of the O atoms. Contours at intervals of 0·1 e $Å^{-3}$; negative contours are dashed and positive are fully drawn.

since they are not thermally smeared. The densities are calculated relative to V^{2+} and neutral O and H atoms in their respective ground states, using the same contracted basis set as in the molecular calculation. Close to vanadium we see a clear buildup of density corresponding to the non-bonding *d* orbital ($1b_2$) and a depletion in the directions of the water ligands. The oxygen lone pairs show up with single maxima 0·5 e Å^{-3} in the H—O—H planes and double maxima (0·35 e Å^{-3}) in planes perpendicular to these. Note here again that there is a difference in the arrangement of the water molecules between the experimental and theoretical studies. The O—H bonds also show up nicely in Fig. 6(*b*). The vanadyl V—O bond is on the other hand less pronounced (0·35 e Å^{-3}) than it was expected.

A population analysis (Mulliken, 1955) of the wave function shows a positive vanadium with charge +1·86 e, a negative vanadyl oxygen with charge −0·23 e, and slightly positive water molecules (+0·08 e) with rather negative oxygen ends (−0·90 e). For the vanadyl bond, an overlap population of +0·65 e gives it a certain covalent strength, whereas the bonds between vanadium and the water ligands show a slightly negative overlap population (−0·02 e), indicating a very different kind of binding. Fairly neutral water molecules were also found in experimental studies with Mg, Ni and Cu as central atoms (Maslen, Ridout & Watson, 1988; Maslen, Watson & Moore, 1988). The charges found for oxygen in those studies were, however, also close to zero, which is not the case for the present theoretical results.

The peaks for the non-bonding *d* orbital are found at much higher values in the theoretical calculations

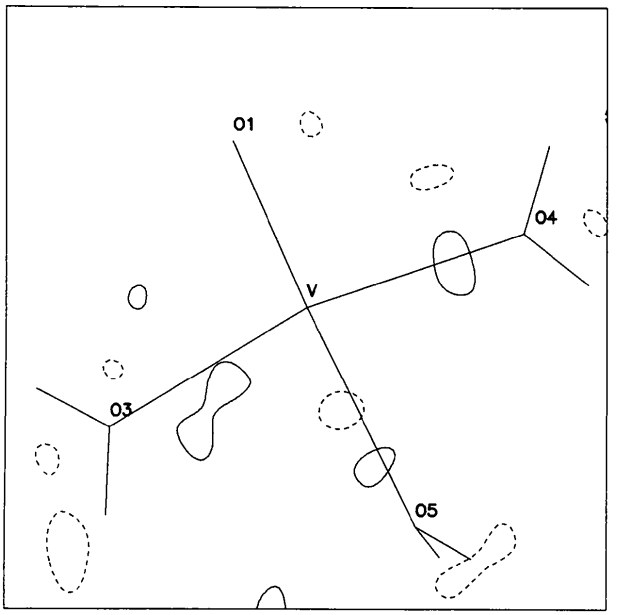

Fig. 5. Residual density corresponding to Fig. 4(*c*). This is calculated as $\rho_{obs} - \rho_{def}$, where ρ_{obs} is the density calculated with the observed structure factors and ρ_{def} the density calculated from the extended deformation model.

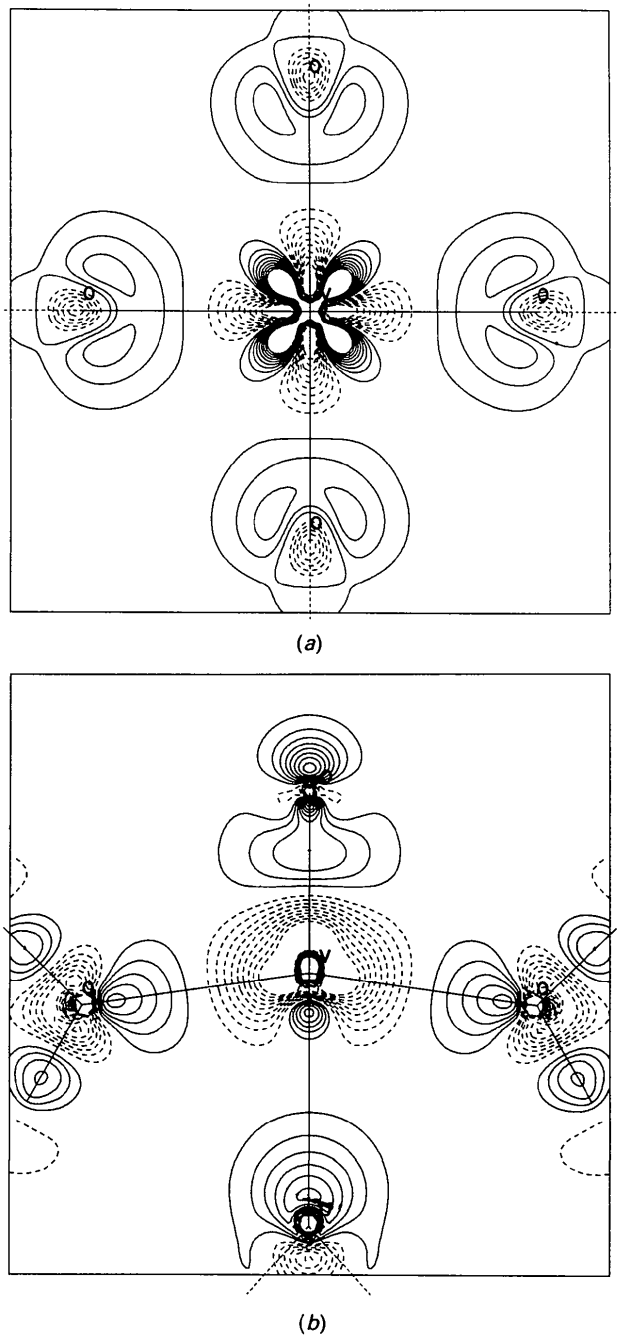

Fig. 6. Theoretical deformation density (*a*) in a plane perpendicular to the V—O bond through the V atom, and (*b*) in a plane containing the V—O bond and two of the equatorial ligands. The deformation is calculated relative to V^{2+} and neutral O and H atoms. Contours as in Fig. 4.

than in the experimental investigation, and they are located much closer to the central atom (0·35 *versus* 0·82 Å). This is again due to the thermal smearing of the experimental densities, and similar differences have been seen in many other studies. Qualitatively the two investigations do, however, compare reasonably well as far as bonds, lone pairs and the non-bonding *d* orbital are concerned. The dense positive peak found close to the central atom in the experiment is not matched by the theoretical results; it is probably caused by experimental errors and series-termination effects. There is a peak in the direction of the axial water ligand, but it is questionable whether this can account for the experimental peak. The negative region on the vanadyl V—O bond close to vanadium is, on the other hand, well reproduced.

References

ABRAHAMS, S. C. (1974). *Acta Cryst.* B**30**, 261–268.

BREITENSTEIN, M., DANNÖHL, H., MEYER, H., SCHWEIG, A. & ZITTLAU, W. (1982). *Electron Distribution and the Chemical Bond*, edited by P. COPPENS & M. B. HALL, pp. 255–281. New York: Plenum Press.

HALL, M. B. (1986). *Chem. Scr.* **26**, 389–394.

HANSEN, N. K. & COPPENS, P. (1978). *Acta Cryst.* A**34**, 909–921.

HERMANSSON, K. (1985). *Acta Cryst.* B**41**, 161–169.

International Tables for X-ray Crystallography (1974). Vol. IV. Birmingham: Kynoch Press. (Present distributor Kluwer Academic Publishers, Dordrecht.)

JOHANSEN, H. (1976). *Acta Cryst.* A**32**, 353–355.

JOHANSEN, H. (1986). *MOLPLOT*. Contour plotting program. Technical Univ. of Denmark.

JOHANSEN, H. & TANAKA, K. (1985). *Chem. Phys. Lett.* **116**, 155–159.

KURKI-SUONIO, K. (1977). *Isr. J. Chem.* **16**, 115–123.

LUNDGREN, J.-O. (1985). *Crystallographic Computer Programs*. Report UUIC-B13-4-06D. Institute of Chemistry, Univ. of Uppsala, Sweden.

MCCANDLISH, L. E., STOUT, G. H. & ANDREWS, L. C. (1975). *Acta Cryst.* A**31**, 245–249.

MASLEN, E. N., RIDOUT, S.C. & WATSON, K. J. (1988). *Acta Cryst.* B**44**, 96–101.

MASLEN, E. N., WATSON, K. J. & MOORE, F. H. (1988). *Acta Cryst.* B**44**, 102–107.

MULLIKEN, R. S. (1955). *J. Chem. Phys.* **23**, 1833–1840.

NORRESTAM, R. (1976). *CADABS*. Program for CAD-4 absorption correction. Technical Univ. of Denmark.

REES, B. (1978). *Acta Cryst.* A**34**, 254–256.

TACHEZ, M. & THÉOBALD, F. (1980*a*). *Acta Cryst.* B**36**, 249–254.

TACHEZ, M. & THÉOBALD, F. (1980*b*). *Acta Cryst.* B**36**, 1757–1761.

TACHEZ, M., THÉOBALD, F., WATSON, K. J. & MERCIER, R. (1979). *Acta Cryst.* B**35**, 1545–1550.

THÉOBALD, F. & GALY, J. (1973). *Acta Cryst.* B**29**, 2732–2736.

TORIUMI, K. & SAITO, Y. (1983). *Adv. Inorg. Chem. Radiochem.* **27**, 27–81.

Acta Cryst. (1990). B**46**, 7–23

Classification of Structures with Anionic Tetrahedron Complexes using Valence-Electron Criteria

BY E. PARTHÉ AND B. CHABOT

Laboratoire de Cristallographie aux Rayons X, Université de Genève, 24 quai Ernest Ansermet, CH-1211 Genève 4, Switzerland

(*Received* 25 *May* 1989; *accepted* 4 *July* 1989)

Abstract

A classification is proposed for the structures of $C_mC'_{m'}A_n$ compounds which contain anionic tetrahedron complexes formed with all the C' and A atoms, the C' atoms centering the tetrahedra, and with the C atoms outside the complex. The classification is based on the observation that compounds with these structures can be considered as general valence compounds, which permits the use of the generalized $(8-N)$ rule. The parameters considered are: (*a*) VEC_A, the partial valence-electron concentration with respect to the anion A, calculated from the position of the elements in the Periodic Table; (*b*) $AA(n/m')$ or $C'C'$ (this depends on the VEC_A value) which correspond to the average number of electrons per tetrahedron available for bonds between anions or between central atoms (and/or for electron lone pairs on the central atom), respectively; and finally (*c*) $C'AC'$ which expresses the average number of C'—A—C' links originating from a tetrahedron. Using simple rules it is possible to calculate the most probable value for $C'AC'$ without knowing the structure. Based on these parameters, classification codes are proposed, written as ${}^{AA(n/m')}VEC_A/C'AC'$, ${}^{0}8/C'AC'$ or ${}^{C'C'}VEC_A/C'AC'$ depending on the VEC_A value. Each of these codes expresses an average of the heteronuclear and homonuclear bonds in the anionic tetrahedron complex. Base tetrahedra can be defined for particular sets of VEC_A, $C'AC'$ and $AA(n/m')$ or $C'C'$ values. All tetrahedron complexes are interpreted as a linkage of one or more

0108-7681/90/010007-17$03.00